Received: 3 August 2021 | Revised: 18 January 2022 | Accepted: 23 January 2022
DOI: 10.1002/aic.17631

AIChE JOURNAL

RESEARCH ARTICLE

Thermodynamics and Molecular-Scale Phenomena

Cuprous-based composite ionic liquids for the selective absorption of CO: Experimental study and thermodynamic analysis

Duan-Jian Tao | **Xue-Cong An** | **Zi-Teng Gao** | **Zhang-Min Li** | **Yan Zhou**

Key Laboratory of Fluorine and Silicon for Energy Materials and Chemistry of Ministry of Education, College of Chemistry and Chemical Engineering, Jiangxi Normal University, Nanchang, Jiangxi, China

Correspondence
Duan-Jian Tao, Key Laboratory of Fluorine and Silicon for Energy Materials and Chemistry of Ministry of Education, College of Chemistry and Chemical Engineering, Jiangxi Normal University, Nanchang, Jiangxi 330022, China.
Email: djtao@jxnu.edu.cn

Funding information
The Key Research and Development Program of Jiangxi Province, Grant/Award Number: 20202BBGL73118; the National Natural Science Foundations of China, Grant/Award Number: 22068013; the Natural Science Foundations of Jiangxi Province, Grant/Award Number: 20192ACBL20025

Abstract

Three cuprous-based composite ionic liquids (ILs) [EimH][OAc]–xCuOAc ($x = 0.5, 0.6, 0.7$) were prepared and employed for efficient absorption of CO. It is shown that the cuprous composite IL [EimH][OAc]–0.6CuOAc exhibited the largest absorption capacity for CO (0.031 g/g at 293.15 K and 1 bar) and had a record CO/N_2 selectivity of 967, which is better than most of common ILs and solvents reported in the literature. The results of Fourier transform infrared (FTIR) spectra, electrospray ionization mass spectrometry (ESI-MS) analysis, and theoretical calculations reveal that such superior CO capacity mainly resulted from two kinds of chemical interaction between CO and the active anionic species $[Cu(OAc)_2]^-$ in [EimH][OAc]–0.6CuOAc. Furthermore, a "deactivated IL model" was further proposed to accurately describe the absorption behavior of CO in [EimH][OAc]–0.6CuOAc, in which the thermodynamic parameters including Henry's law constants, reaction equilibrium constants, and absorption enthalpies were estimated by the correlation of the experimental solubilities of CO.

KEYWORDS
absorption, carbon monoxide, cuprous, ionic liquids, thermodynamic model

1 | INTRODUCTION

As a typical small-molecule gas, carbon monoxide (CO) is used as an important raw material for C1 chemistry.[1,2] Also, CO is one of the sources of environmental pollution. Nowadays, a huge amount of CO is generated and exhausted in tail gases such as synthesis gas, yellow phosphorus tail gas, calcium carbide furnace gas, coke oven gas, and blast furnace gas.[3] In China, more than 15 million tons of CO from blast furnace gas is produced annually.[4] Thus, it is believed that the capture and recovery of CO from those tail gases has become an important research topic in the fields of environment protection and chemical industry.

Ionic liquids (ILs) are considered as a type of state-of-the-art solvents for gas absorption thanks to their task-specific properties such as extremely low volatility, good solvability, high thermal stability, and tunable designability.[5,6] So far, many varieties of ILs have been served as wonderful solvents for efficient absorption of acid gases including CO_2,[7] SO_2,[8] and NO_x.[9] However, compared with those acid gases, CO has the higher bond dissociation energy and thereby results in low solubilities in normal ILs.[10–12] For example, Wu and his coworkers[13] prepared a cuprous protic IL [TEA][$CuCl_2$] for absorption of CO and obtained the solubility of 0.078 mol CO per mol IL at 303.15 K and 1 bar. Tao and his co-workers[14] reported that the CO uptake capacity of a cuprous-based IL [EimH][$CuCl_2$] was 0.158 mol CO per mol IL at 293.15 K and 1 bar. Up to now, the current research results had shown that the solubilities of CO in these reported ILs remained very small. The screening of ILs absorbent for efficient absorption of CO is still in high demand.

As well known, separation and recovery of CO from syngas using the CuCl π-complexation adsorbent in a pressure swing adsorption

https://doi.org/10.1002/aic.17631

process (PSA) was commercialized about 30 years ago.[15,16] However, it is worth pointing out that the competitive gas N_2 is often together with CO in many tail gases. Although various CuCl π-complexation adsorbents had been developed for efficiently recovering CO, the abundant pores and large specific surface areas in these π-complexation adsorbents also leaded to considerable N_2 adsorption capacities. As a result, many types of CuCl π-complexation adsorbents suffered from unsatisfied CO/N_2 separation selectivity.[17–19] Thus, highly selective absorption of CO from N_2 is another requirement for developing an advanced CO absorption process. In addition, in comparison to solid adsorption, liquid absorption is a promising alternative process for CO capture. Pumping can allow liquid absorption in a continuous process, whereas solid adsorbents are usually used in batch processes with low efficiency.

Herein, three cuprous-based composite ILs were prepared by the incorporation of cuprous acetate (CuOAc) into the IL 1-ethylimidazole hydroacetate ([EimH][OAc]) with different molar ratios. Then the performance of cuprous-based composite ILs for selective absorption of CO from N_2 was investigated in detail, and their density and viscosity values were also determined. Moreover, the Fourier transform infrared (FTIR) spectra and quantum mechanical calculations of cuprous-based composite ILs before and after CO uptake were conducted to identify the interaction mechanism. In addition, a "deactivated IL model" was also proposed to carry out the thermodynamic analysis, and the thermodynamic parameters can be estimated by the correlation of the temperature dependence of CO solubility.

2 | EXPERIMENTAL

2.1 | Materials

1-Ethylimidazole hydroacetate ([EimH][OAc], ≥99%), 1-ethyl-3-methylimidazolium acetate ([Emim][OAc], high purity of 99%), and 1-ethylimidazole hydrochloride ([EimH]Cl, high purity of 99%) were supplied by the Centre of Green Chemistry and Catalysis, LICP, CAS. CuOAc (high purity of 97%) and cuprous chloride (CuCl, high purity of 99%) were obtained from Adamas (Shanghai, Adamas-Beta). Gases such as N_2 and CO (≥99.99%) were purchased from Jiangxi Huate Special Gas Co., Ltd. The other reagents were obtained commercially and used directly.

2.2 | Synthesis of cuprous-based composite ILs

The cuprous-based composite ILs were prepared by easily mixing of [EimH][OAc] and CuOAc with the molar ratios of 1:0.5, 1:0.6, and 1:0.7, respectively. Take the preparation of [EimH][OAc]–0.6CuOAc as an example, the raw materials [EimH][OAc] and CuOAc were mixed with a mole ratio of 1:0.6, and the mixture was stirred at 298.3 K for 1 h. Then the cuprous-based composite IL [EimH][OAc]–0.6CuOAc was obtained.

The water content of cuprous-based composite ILs was examined by a Karl Fisher titration, and the results were lower than 0.05%. Densities and viscosities of cuprous-based composite ILs were measured on an Anton Paar DMA 4500 automatic densitometer and cone-plate viscometer (Brookfield DV II + Pro), respectively. FTIR spectra was carried out on a NEXUS870 spectrometer. Electrospray ionization mass spectrometry (ESI-MS) were examined on an Agilent1290/maX impact instrument with negative ion mode.

2.3 | Gas solubility measurements

The measurement of CO and N_2 uptake was carried out on a dual-chamber volumetric apparatus, which was the same as our previous study (Figure S1). The measurements principle is through the gas content in the gas reservoir subtracting the surplus of the gas content in the equilibrium cell equals the uptake of the IL absorbent.[20,21] Triplicate experiments were examined for each IL for obtaining averaged values. More details information can be found in the Supporting Information. After the completion of CO absorption, the CO-saturated IL was treated at 353.15 K under a vacuum of 0.01 bar with 2 h to desorb CO. Then the regenerated IL was used for CO absorption in the next run.

3 | RESULTS AND DISCUSSION

3.1 | Physical properties

The densities and viscosities data of liquid absorbent are fundamental physical properties for the devise of gas absorption process.[22–24] As shown in Figure 1, the densities and viscosities values of three cuprous-based composites ILs at 293.15–353.15 K. The sequence of density was as follows: [EimH][OAc]–0.7CuOAc > [EimH][OAc]–0.6CuOAc > [EimH][OAc]–0.5CuOAc. This indicates that the density value of cuprous-based composite IL enhanced with increasing the amount of CuOAc. Similarly, the viscosity of these three cuprous-based composite ILs had the same changing tendency. The more CuOAC loads, the viscosity value increases. Moreover, it can be seen that the density value decreased linearly and the viscosity decreased exponentially with the temperature increased. Then the density and viscosity for the present cuprous-based composite ILs were fitted by the following Equations (1) and (2),[25,26] respectively. The fitted parameters are summarized in Table S1.

$$\rho = A + BT \tag{1}$$

$$\eta = \eta_0 \times \exp\left(\frac{C}{T - T_0}\right) \tag{2}$$

3.2 | CO absorption capacity

Absorption capacities and kinetics are two important indexes to CO capture. Figure 2 shows the CO absorption rates by the cuprous-based composite ILs at 293.15 K and 1 bar. It is found that the amount of

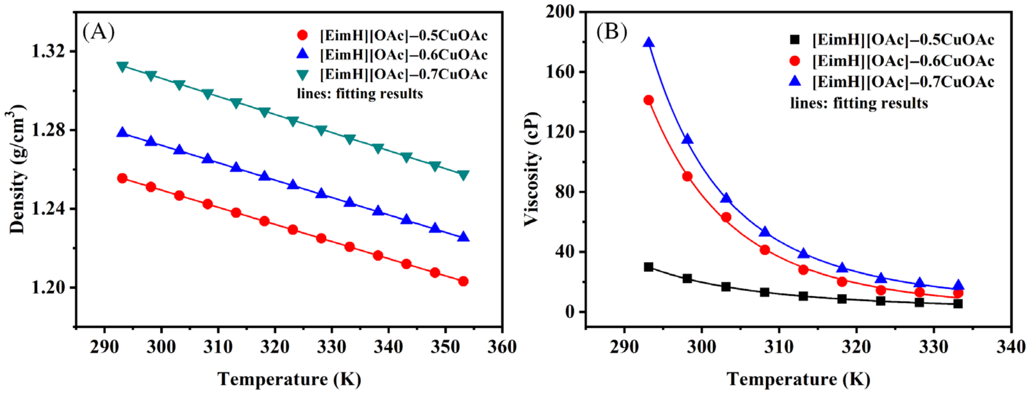

FIGURE 1 Densities (A) and viscosities (B) of cuprous-based composite ILs [EimH][OAc]–*x*CuOAc. ILs, ionic liquids

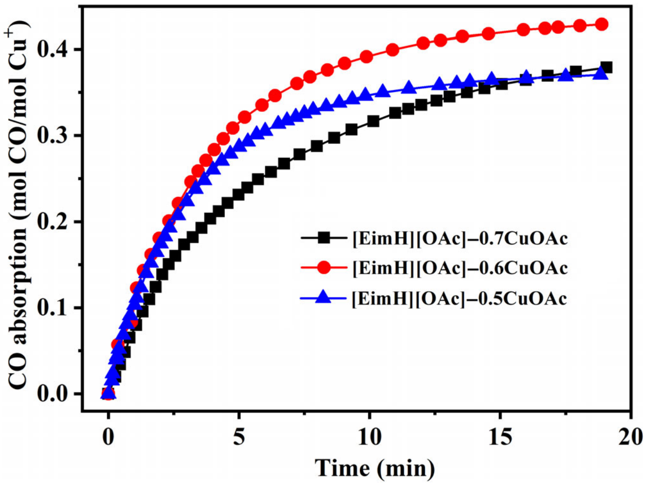

FIGURE 2 CO absorption rate for cuprous-based composite ILs [EimH][OAc]–*x*CuOAc at 293.15 K and 1 bar. ILs, ionic liquids

CuOAc had an obvious impact on the CO uptake. The cuprous-based composite IL [EimH][OAc]–0.6CuOAc shows the highest CO uptake of 0.45 mol mol^{-1} compared with [EimH][OAc]–0.5CuOAc and [EimH][OAc]–0.7CuOAc. Moreover, these three cuprous-based composite ILs could absorb ~70% of saturated CO absorption capacity at 293.15 K and 1 bar within 5 min and achieve absorption equilibrium within 20 min. Additionally, the viscosity of [EimH][OAc]–0.6CuOAc after CO absorption had not increased too much compared with the previous reference ILs (Figure S2, Table S1), which accounts for the excellent CO uptake rate. This finding demonstrates that all the cuprous-based composite ILs exhibited satisfactory CO absorption rates.

Inspired by these dramatic results, a series of reference absorbents [EimH][OAc], CuOAc, [Emim][OAc]–0.6CuOAc, and [EimH]Cl–0.6CuCl were further designed and employed for CO absorption to clarify the outstanding performance of [EimH][OAc]–0.6CuOAc. The results are listed in Table 1. This demonstrates that the IL [EimH][OAc] had no absorption capacity of CO, showing that the presence of Cu$^+$ dominates CO sorption (Table 1, entries 1, 2). Also, an aprotic IL [Emim][OAc]–0.6CuOAc was synthesized and used for absorption of CO. Its solubility was only 0.07 mol mol^{-1} at 293.15 K and 1 bar, which is significantly lower than that of [EimH][OAc]–0.6CuOAc (Table 1, entries 1, 3). It is indicated that the protonated cation ([EimH]$^+$) plays an important function in such excellent CO solubility.[14] Moreover, the cuprous chloride-based IL [EimH]Cl–0.6CuCl was found to have the CO uptake of 0.13 mol mol^{-1} (Table 1, entry 4), which is greatly inferior to [EimH][OAc]–0.6CuOAc (0.45 mol mol^{-1}). This suggests that the acetate anion is also beneficial for the absorption of CO.

Moreover, the influence of pressure and temperature on the capture of CO by [EimH][OAc]–0.6CuOAc were studied. As expected, the CO uptake improved to 0.50 mol mol^{-1} under the pressure of 2 bar (Table 1, entry 5). As the partial pressure is reduced from 1 bar to 0.1 and 0.02 bar, the CO absorption capacity could retain 0.23 and 0.12 mol mol^{-1} (Table 1, entries 6, 7), respectively, demonstrating the considerable CO absorption ability of [EimH][OAc]–0.6CuOAc under low pressure. Also, the CO uptake of [EimH][OAc]–0.6CuOAc declined slightly with the increase of the temperature from 293.15 to 313.15 K (Table 1, entries 8, 9). Furthermore, Table 2 lists the CO uptake of the previously reported absorbents including known ILs and organic solvents. The comparison results show that the cuprous-based composite IL [EimH][OAc]–0.6CuOAc had much higher absorption than common organic solvents and most ILs such as [hmim][CuCl$_2$],[12] [TEA][CuCl$_2$],[13] [P$_{4448}$][Pen],[20] [BimH]Cl-CuCl-1.0ZnCl$_2$,[27] and [HDEEA][Cl] + CuCl + EG (1:1:4)[28] in terms of CO capacity either in molar ratio or mass ratio.

3.3 | CO absorption selectivity

Since CO and N$_2$ often present in most tail gases, it is necessary and demand for highly selective capture of CO from N$_2$.[16] Then the capacity of N$_2$ in the cuprous-based composite IL [EimH][OAc]–0.6CuOAc at 293.15 K and 1 bar was measured and found to be 7.7×10^{-4} mol N$_2$ per mol IL. This suggests that compared to efficient absorption of CO, [EimH][OAc]–0.6CuOAc showed extremely low capacities for capturing N$_2$. Moreover, the absorption amount

TABLE 1 Summary of CO absorption capacities for different absorbents

Entry	Absorbents	Conditions	CO absorption capacity (mol CO/mol Cu^+)	CO absorption capacity (g CO/g absorbent)
1	[EimH][OAc]–0.6CuOAc	293.15 K, 1 bar	0.45	0.031
2	[EimH][OAc]	293.15 K, 1 bar	–	–
3	[Emim][OAc]–0.6CuOAc	293.15 K, 1 bar	0.07	4.8×10^{-3}
4	[EimH]Cl–0.6CuCl	293.15 K, 1 bar	0.13	0.011
5	[EimH][OAc]–0.6CuOAc	293.15 K, 2 bar	0.50	0.037
6	[EimH][OAc]–0.6CuOAc	293.15 K, 0.1 bar	0.23	0.017
7	[EimH][OAc]–0.6CuOAc	293.15 K, 0.02 bar	0.12	0.009
8	[EimH][OAc]–0.6CuOAc	303.15 K, 1 bar	0.39	0.028
9	[EimH][OAc]–0.6CuOAc	313.15 K, 1 bar	0.33	0.024

TABLE 2 Comparison of CO absorption capacities in cuprous-based composite ILs with previously reported absorbents

Absorbents	Temperature (K)	Pressure (bar)	CO absorption capacity (mol CO/mol Cu^+)	CO absorption capacity (g CO/g absorbent)	References
[EimH][OAc]–0.6CuOAc	293.15	1.0	0.45	0.031	This study
[EimH][$CuCl_2$]	293.15	1.0	0.157	0.019	14
[TEA][$CuCl_2$]	303.15	1.0	0.078	9.2×10^{-3}	13
[P_{4448}][Pen]	303.15	1.0	0.046	3.1×10^{-3}	20
[hmim][$CuCl_2$]	303.15	1.0	0.02	1.9×10^{-3}	12
[BimH]Cl–CuCl–1.0$ZnCl_2$	353.15	1.0	0.075	5.3×10^{-3}	27
[HDEEA][Cl] + CuCl + EG (1:1:4)	293.15	1.0	0.203	0.011	28
[Bmim][Tf_2N]	303.15	1.0	1.5×10^{-3}	1.0×10^{-4}	11
[Bmim][PF_6]	295.15	1.0	3.0×10^{-3}	3.0×10^{-4}	10

Abbreviation: ILs, ionic liquids.

ratio of CO and N_2 on various ILs and adsorbent materials at 1 bar was further compared, and the results are presented in Figure 3. It is demonstrated that the CO/N_2 absorption amount ratio for [EimH][OAc]–0.6CuOAc reached a record value of 967 at 293.15 K and 1 bar, which is much higher than many ILs[12–14,20,27] and most porous MOFs adsorbent materials.[29–32] The ultralow N_2 capacity plus superior CO uptake in [EimH][OAc]–0.6CuOAc contributes to the highest CO/N_2 ideal separation selectivity. In addition, the solubility of pure H_2 in [EimH][OAc]–0.6CuOAc at 293.15 K and 1 bar was found be as low as 4.5×10^{-3} mol H_2 per mol IL. Therefore, it is well accepted that the cuprous-based composite IL [EimH][OAc]–0.6CuOAc would be a good substitute for the selective capture and recovery of CO from N_2 and H_2 in tail gas.

3.4 | CO absorption mechanism

Figure 4 shows the absorption isotherm of CO in [EimH][OAc]–0.6CuOAc at temperatures ranging from 293.15 to 323.15 K and pressures from 0.01 to 3 bar. It is demonstrated that the absorption capacity of CO increased sharply at low CO partial pressure from 0.01

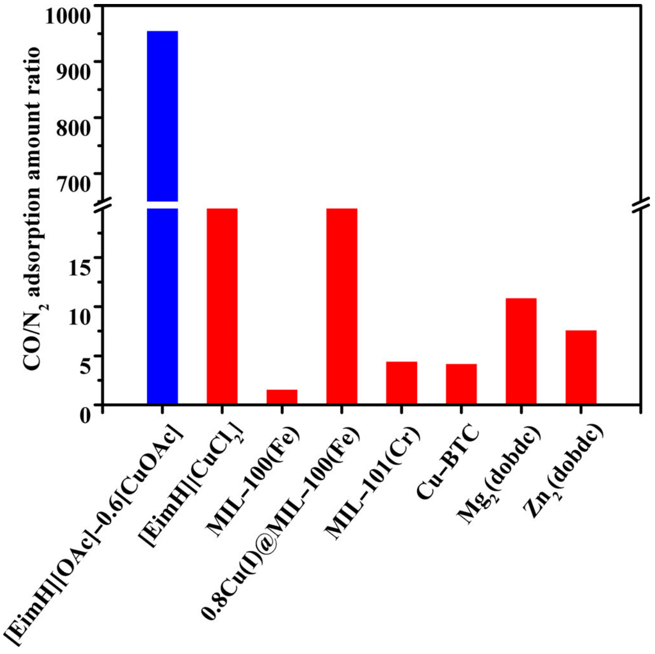

FIGURE 3 The comparison of CO/N_2 adsorption amount ratio of various adsorbents at 1.0 bar

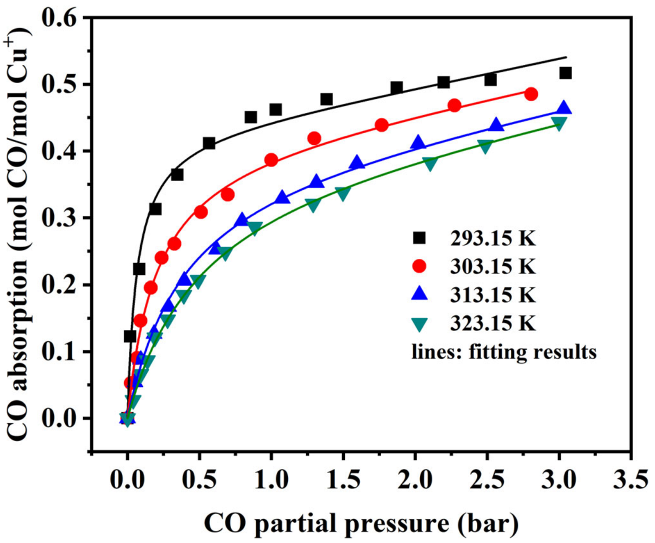

FIGURE 4 Solubilities of CO in [EimH][OAc]–0.6CuOAc at different temperatures

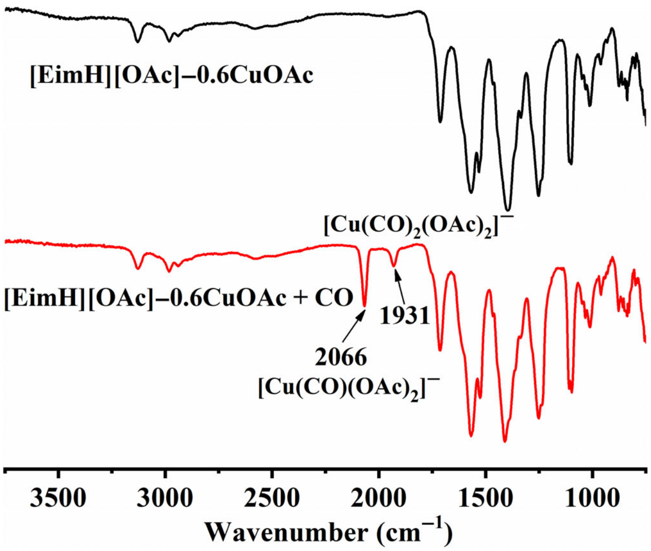

FIGURE 5 FTIR spectra of [EimH][OAc]–0.6CuOAc before and after CO absorption. FTIR, Fourier transform infrared

to 0.5 bar, and further raised linearly with an increase of CO partial pressure from 1 to 3 bar. This indicates that the CO dissolution behavior in [EimH][OAc]–0.6CuOAc strongly deviates from the ideality, particularly in the low-pressure area. By contrast, most of known cuprous ILs and normal ILs only had the physical interaction with CO, in which the CO uptake increased linearly with rising CO partial pressure.[14,27] Therefore, it is speculated that except for physical absorption, a chemisorption interaction would also take place between CO and [EimH][OAc]–0.6CuOAc.

Subsequently, the analysis of anion species in [EimH][OAc]–0.6CuOAc by the ESI-MS with negative ion mode was investigated to disclose the active species for capturing CO. It is seen from Figure S3, the complex anion [Cu(OAc)$_2$]$^-$ was mainly detected in the cuprous-based composite IL [EimH][OAc]–0.6CuOAc, which is considered to be the active site for CO absorption. Figure 5 shows the FTIR spectra of [EimH][OAc]–0.6CuOAc before and after CO absorption. It can be seen that two new peaks at 2066 and 1931 cm^{-1} were observed after [EimH][OAc]–0.6CuOAc absorbing CO, which belongs to the CO stretching vibrations in the complex of [Cu(CO)(OAc)$_2$]$^-$ and [Cu(CO)$_2$(OAc)$_2$]$^-$, respectively. The captured CO in [EimH][OAc]–0.6CuOAc had the large red shift higher than free CO with the vibrational frequency of 2143 cm^{-1} and [EimH][OAc]–0.6CuOAc would have a strong chemical interaction for CO capture, making a good agreement with the previous literature reported by Wu et al.[13] Therefore, it is demonstrated that the Cu$^+$ sites of [Cu(OAc)$_2$]$^-$ in ILs absorbents can preferentially capture CO through π-complexation interaction. This π-complexation interaction has also been employed for the capture of CO by various Cu$^+$-containing solid adsorbents.[31,32]

To further disclose the interaction of the anion [Cu(OAc)$_2$]$^-$ with CO, density functional theory (DFT) calculations were carried out with Gaussian 16 at the B3LYP/6–311 + G level (Figure 6). When the anion [Cu(OAc)$_2$]$^-$ complexed with one CO molecular, the bond length of Cu—O bond increased from 1.868 to 2.007 Å and the complex [Cu(CO)(OAc)$_2$]$^-$ had a negative absorption enthalpy $\Delta H_{\text{cal-1}}$ of −39.1 kJ/mol. Moreover, when the anion [Cu(OAc)$_2$]$^-$ complexed with the two CO molecules, the complex [Cu(CO)$_2$(OAc)$_2$]$^-$ had more negative absorption enthalpy $\Delta H_{\text{cal-2}}$ of −61.3 kJ/mol and the bond length of Cu—O bond further had been enlarged to 2.038 Å. This finding demonstrates that the formation of the complex [Cu(CO)$_2$(OAc)$_2$]$^-$ with the more negative enthalpy was energetically favored. These two kinds of interaction are consistent with the result of FTIR spectra. Both of these calculated binding energies between [Cu(OAc)$_2$]$^-$ and CO are much stronger than the H-bonding interaction (∼−10 kJ/mol), verifying the presence of CO chemisorption by [EimH][OAc]–0.6CuOAc. Therefore, the cuprous-based composite IL [EimH][OAc]–0.6CuOAc affords two kinds of chemical interactions for absorbing CO and results in both extremely high CO capacity and absorption selectivity.

3.5 | Thermodynamic analysis

To get insight into the dissolution behavior of CO in [EimH][OAc]–0.6CuOAc, a “deactivated IL model”[33,34] is employed to correlate the CO solubility data in mol mol^{-1}. The detailed derivation of the “deactivated IL model” is provided in the Supporting Information. As shown in Equations (3)–(5), it assumes that the physical dissolution of CO in the cuprous-based composite IL occurs, and CO reacts with the cuprous-based composite IL by 1:1 and 1:2 mechanisms, respectively. Equation (6) is the “deactivated IL” model in which Z is the moles of CO (including both physical dissolution and chemical absorption) divided by the moles of IL. P_{CO} is that the CO partial pressure in bar, H donates the Henry's constant in bar. K_1 and K_2 represent the equilibrium constant, and C is the molar ratio of active IL to whole IL.

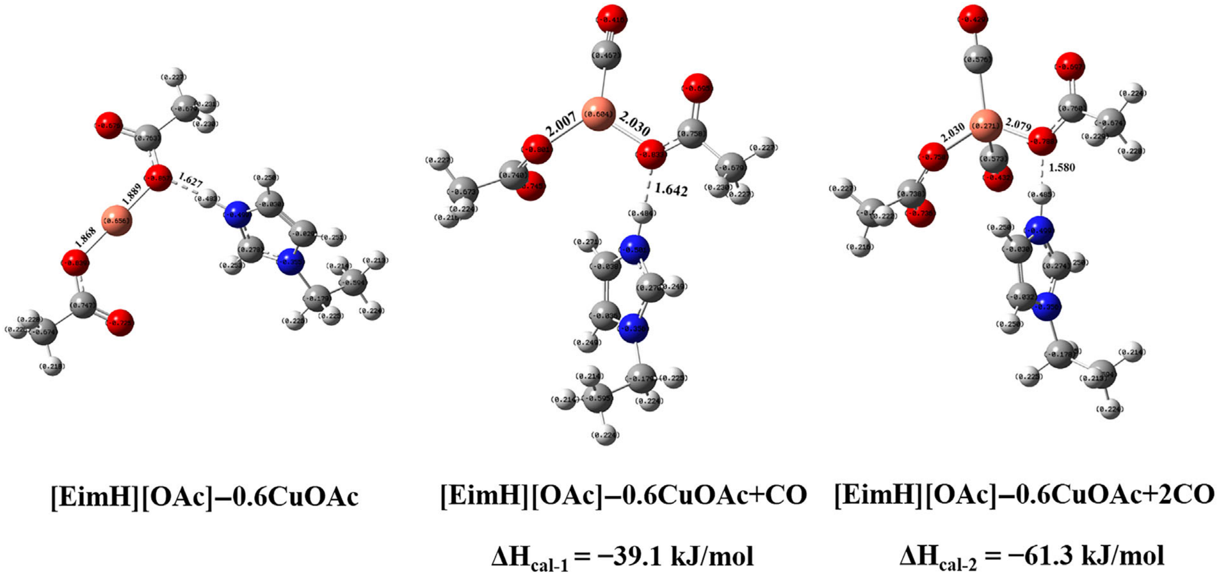

FIGURE 6 The anion specie $[CuOAc_2]^-$ in [EimH][OAc]–0.6CuOAc and their complexes with CO. Cu: brown red, O: red, N: blue, C: gray, H: white

$$CO_{(g)} \rightleftharpoons CO_{(l)} \tag{3}$$

$$CO_{(g)} + [Cu(OAc)_2]^- \rightleftharpoons [Cu(CO)(OAc)_2]^- \tag{4}$$

$$2CO_{(g)} + [Cu(OAc)_2]^- \rightleftharpoons [Cu(CO)_2(OAc)_2]^- \tag{5}$$

$$Z = \frac{P_{CO}/H}{1-P_{CO}/H} + \frac{K_1 P_{CO} + K_2 P_{CO}^2}{1 + K_1 P_{CO} + K_2 P_{CO}^2} C \tag{6}$$

There are four unknown parameters in Equation (6), H, K_1, K_2, and C. These four parameters were correlated and acquired by fitting the experimental data. The fitting curves are illustrated in Figure 4. It can be seen that the experimental absorption of CO in the cuprous-based composite IL [EimH][OAc]–0.6CuOAc can be well correlated using Equation (6), and all the correlation coefficients R^2 are higher than 0.99, showing a good precision of the "deactivated IL model." Then the fitted parameters H, K_1, K_2, and C are summarized in Table 3. It is showed that the increase of temperature caused increasing the Henry's law constant H but decreased the values of K_1 and K_2. This means that a larger H or a smaller K corresponds to a lower CO solubility, suggesting the favor of a low temperature for the absorption of CO.

Based on Equation (6) and the estimated thermodynamic parameters in Table 3, the physical and chemical absorption profiles of CO in the cuprous-based composite IL [EimH][OAc]–0.6CuOAc at 293.15 K were further calculated to clarify the respective contributions of physical solubility and chemical capacity to the total solubility of CO. As seen from Figure 7, it is shown that the chemical absorption capacity increased significantly at the pressure from 0 to 0.5 bar and approached to a flat at the pressures higher than 0.5 bar because of the limitation of chemical equilibrium reaction. By contrast, the physical solubility increased linearly with the increase of CO pressure and

TABLE 3 Thermodynamic parameters for the absorption of CO by [EimH][OAc]–0.6CuOAc calculated from the deactivated IL model

	T (K)			
Parameter	**293.15**	**303.15**	**313.15**	**323.15**
H	28.98	30.54	31.84	32.19
C	0.43	0.41	0.40	0.39
K_1	0.33	0.25	0.21	0.18
K_2	14.86	4.77	2.33	1.79

Abbreviation: IL, ionic liquid.

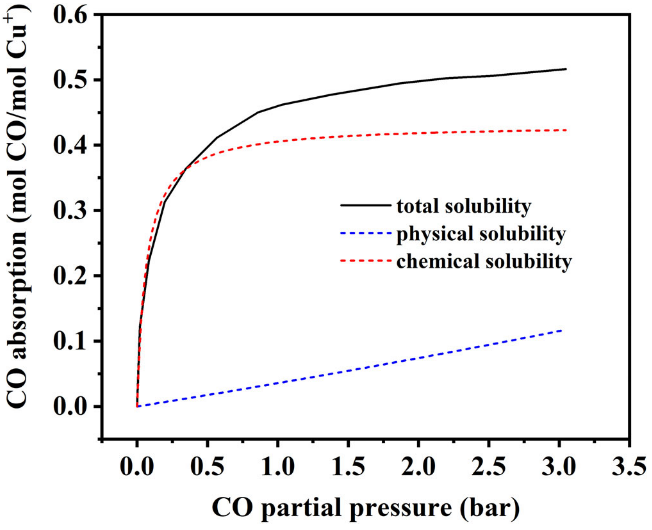

FIGURE 7 Chemical and physical solubility of CO in [EimH][OAc]–0.6CuOAc at 293.15 K calculated by the deactivated IL model. IL, ionic liquid

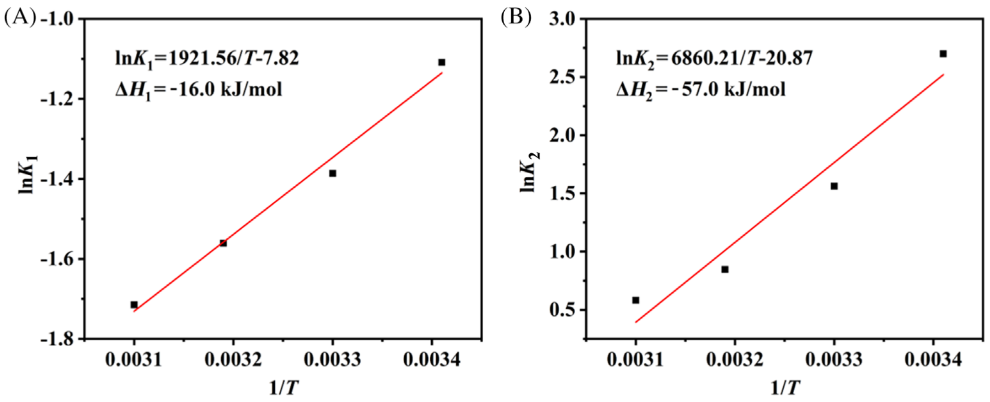

FIGURE 8 Linear fit of ln *K* and 1/*T* for CO absorption in [EimH][OAc]–0.6CuOAc

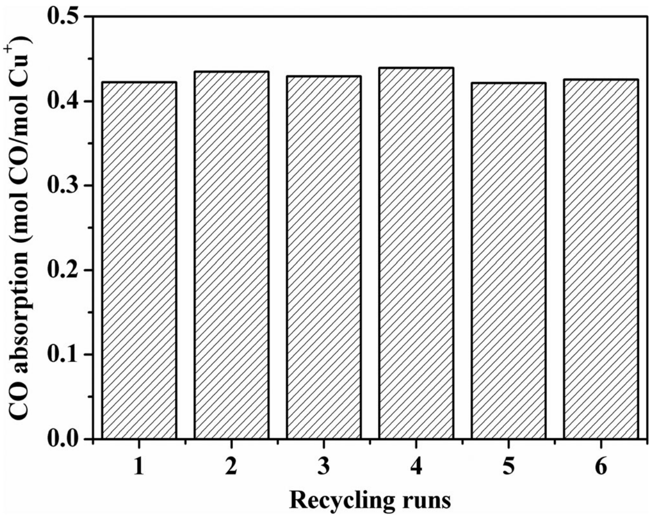

FIGURE 9 Recycle performance of [EimH][OAc]–0.6CuOAc for CO absorption

yet the quantity was very low. Therefore, it is demonstrated that the chemical absorption accounts for the main part of the total CO absorption capacity during the whole process.

In addition, the experimental enthalpies (ΔH_1, ΔH_2) for reaction Equations (4) and (5) were computed from the van't Hoff equation.[35] Similarly, the enthalpy of solution ΔH_{sol} that reflects the thermal effect of physical dissolution of CO was also calculated using Equation (8).

$$\frac{\partial \ln K}{\partial T} = \frac{\Delta H}{RT^2} \tag{7}$$

$$\frac{\partial \ln H}{\partial T} = -\frac{\Delta H_{sol}}{RT^2} \tag{8}$$

The calculated results are shown in Figure 8. ΔH_1 and ΔH_2 are found to be −16.0 and −57.0 kJ/mol, respectively. The value of ΔH_2 for the reaction Equation (5) agrees well with the calculated binding energy $\Delta H_{cal\text{-}2}$ between $[Cu(OAc)_2]^-$ and two CO molecules, which is much larger than the calculated binding energy $\Delta H_{cal\text{-}1}$ of $[Cu(OAc)_2]^-$ with one CO molecular. It implies that the interaction of the anion $[Cu(OAc)_2]^-$ with two CO molecules to form the complex $[Cu(CO)_2(OAc)_2]^-$ is thermodynamically favored, which contributes to a superior CO chemisorption capacity. On the contrary, it is seen from Figure S4 that the value of ΔH_{sol} was only −2.9 kJ/mol, showing the weaker interaction of physical dissolution of CO in [EimH][OAc]–0.6CuOAc and thereby a very low CO physical solubility.

3.6 | Recycle test

To determine the reversible ability of [EimH][OAc]–0.6CuOAc, six absorption-desorption cycles for CO absorption was carried out. It can be seen from Figure 9 that the high CO uptake capacity of the cuprous-based composite IL [EimH][OAc]–0.6CuOAc was well maintained, demonstrating that the absorption of CO is completely reversible. Furthermore, the FTIR characterization of fresh and recycled [EimH][OAc]–0.6CuOAc was compared as illustrated in Figure S5. The FTIR spectra of recycled [EimH][OAc]–0.6CuOAc remained almost unchanged compared with the fresh sample. All the above results demonstrate that the cuprous-based composite IL [EimH][OAc]–0.6CuOAc absorbent shows excellent reusability and stability for the reversible CO absorption process.

4 | CONCLUSIONS

In summary, three cuprous-based composite ILs [EimH][OAc]–*x*CuOAc were successfully prepared and developed for efficient absorption of CO. It is found that the cuprous composite IL [EimH][OAc]–0.6CuOAc showed a very large capacity of 0.031 g CO per gram IL but nearly excluded the absorption of N_2 (7.7×10^{-4} mol N_2 per mol IL), as well as a high ideal selectivity of 967 for CO/N_2 mixture was obtained at 293.15 K and 1 bar. Moreover, the results of FTIR spectra, ESI-MS analysis, and theoretical calculations demonstrate that [EimH][OAc]–0.6CuOAc can afford two kinds of chemical interactions between CO and the active anionic site $[Cu(OAc)_2]^-$ for capturing CO efficiently. The thermodynamic analysis further showed that the development of a deactivated IL model could correlate the absorption behavior of CO in [EimH][OAc]–0.6CuOAc very well, and thermodynamic parameters including Henry's law constants, reaction equilibrium constants, and absorption enthalpies were also obtained. In addition, the cuprous composite IL [EimH][OAc]–0.6CuOAc had excellent reusability in reversible absorption of CO during six absorption−desorption cycles. Therefore, the cuprous-based composite ILs are considered to be an encouraging candidate absorbent for selective absorption of CO from N_2.

ACKNOWLEDGMENTS

We gratefully thank the Key Research and Development Program of Jiangxi Province (20202BBGL73118), the Natural Science Foundations of Jiangxi Province (20192ACBL20025), and the National Natural Science Foundations of China (22068013) for financial support.

AUTHOR CONTRIBUTIONS

Duan-Jian Tao: Conceptualization (lead); formal analysis (lead); project administration (lead); supervision (lead); writing – original draft (lead); writing – review and editing (lead). **Xue-Cong An:** Data curation (equal); formal analysis (equal); investigation (equal); methodology (equal). **Zi-Teng Gao:** Formal analysis (equal); methodology (equal); writing – review and editing (equal). **Zhang-Min Li:** Data curation (equal); methodology (equal); writing – review and editing (equal). **Yan Zhou:** Data curation (equal); methodology (equal); software (equal); supervision (equal).

DATA AVAILABILITY STATEMENT

The data that support the findings of this study are available from the corresponding author upon reasonable request.

ORCID

Duan-Jian Tao https://orcid.org/0000-0002-8835-0341

REFERENCES

1. Brennführer A, Neumann H, Beller M. Palladium-catalyzed carbonylation reactions of aryl halides and related compounds. *Angew Chem Int Ed*. 2009;48(23):4114-4133.
2. Friis SD, Lindhardt AT, Skrydstrup T. The development and application of two-chamber reactors and carbon monoxide precursors for safe carbonylation reactions. *Accounts Chem Res*. 2016;49(4):594-605.
3. Saha D, Deng SG. Adsorption equilibria and kinetics of carbon monoxide on zeolite 5A, 13X, MOF-5, and MOF-177. *J Chem Eng Data*. 2009;54(8):2245-2250.
4. Feng SZ, Jiang F, Wu Z, Wang HM, Ju WM, Wang HK. CO emissions inferred from surface CO observations over China in december 2013 and 2017. *J Geophys Res Atmos*. 2020;125(7):e2019JD031808.
5. Lei ZG, Dai CN, Chen BH. Gas solubility in ionic liquids. *Chem Rev*. 2014;114(2):1289-1326.
6. Dong K, Liu XM, Dong HF, Zhang XP, Zhang SJ. Multiscale studies on ionic liquids. *Chem Rev*. 2017;117(10):6636-6695.
7. Chen FF, Huang K, Zhou Y, et al. Multi-molar absorption of CO_2 by the activation of carboxylate groups in amino acid ionic liquids. *Angew Chem Int Ed*. 2016;55(25):7166-7170.
8. Wang CM, Cui GK, Luo XY, Xu YJ, Li HR, Dai S. Highly efficient and reversible SO_2 capture by tunable azole-based ionic liquids through multiple-site chemical absorption. *J Am Chem Soc*. 2011;133(31):11916-11919.
9. Chen KH, Shi GL, Zhou XY, Li HR, Wang CM. Highly efficient nitric oxide capture by azole-based ionic liquids through multiple-site absorption. *Angew Chem Int Ed*. 2016;55(46):14364-14368.
10. Ohlin CA, Dyson PJ, Laurenczy G. Carbon monoxide solubility in ionic liquids: determination, prediction and relevance to hydroformylation. *Chem Commun*. 2004;9:1070-1071.
11. Gan Q, Zou YR, Rooney D, et al. Theoretical and experimental correlations of gas dissolution, diffusion, and thermodynamic properties in determination of gas permeability and selectivity in supported ionic liquid membranes. *Adv Colloid Interfac*. 2011;164(1):45-55.
12. Zarca G, Ortiz I, Urtiaga A. Kinetics of the carbon monoxide reactive uptake by an imidazolium chlorocuprate(I) ionic liquid. *Chem Eng J*. 2014;252:298-304.
13. Tu ZH, Zhang YY, Wu YT, Hu XB. Self-enhancement of CO reversible absorption accompanied by phase transition in protic chlorocuprate ionic liquids for effective CO separation from N_2. *Chem Commun*. 2019;55(23):3390-3393.
14. Liu YM, Tian ZQ, Qu F, Zhou Y, Liu Y, Tao DJ. Tuning ion-pair interaction in cuprous-based protic ionic liquids for significantly improved CO capture. *ACS Sustain Chem Eng*. 2019;7(13):11894-11900.
15. Xie YC, Zhang J, Qiu J, et al. Zeolites modified by CuCl for separating CO from gas mixtures containing CO_2. *Adsorption*. 1996;3:27-32.
16. Golden TC, Guro DE, Kratz WC, Occhialini JM, Sabram TE. *Fundamentals of Adsorption*. Elsevier; 1998.
17. Zarca G, Ortiz I, Urtiaga A. Copper(I)-containing supported ionic liquid membranes for carbon monoxide/nitrogen separation. *J Membr Sci*. 2013;438:38-45.
18. Sato H, Kosaka W, Matsuda R, et al. Self-accelerating CO sorption in a soft nanoporous crystal. *Science*. 2014;343(6167):167-170.
19. Ma JH, Li L, Ren J, Li RF. CO adsorption on activated carbon-supported cu-based adsorbent prepared by a facile route. *Sep Purif Technol*. 2010;76(1):89-93.
20. Tao DJ, Chen FF, Tian ZQ, et al. Highly efficient carbon monoxide capture by carbanion-functionalized ionic liquids through C-site interactions. *Angew Chem Int Ed*. 2017;56(24):6843-6847.
21. An XC, Li ZM, Zhou Y, Zhu WS, Tao DJ. Rapid capture and efficient removal of low-concentration SO_2 in simulated flue gas by hypercrosslinked hollow nanotube ionic polymers. *Chem Eng J*. 2020;394:124859.
22. Chen FF, Huang K, Fan JP, Tao DJ. Chemical solvent in chemical solvent: a class of hybrid materials for effective capture of CO_2. *AIChE J*. 2018;64(2):632-639.
23. Ma Y, Zhang J, Huang K, Jiang L. Highly efficient and selective separation of ammonia by deep eutectic solvents through cooperative acid-base and strong hydrogen-bond interaction. *J Mol Liq*. 2021;337:116463.
24. Cao Y, Zhang J, Ma Y, Wu W, Huang K, Jiang L. Designing low-viscosity deep eutectic solvents with multiple weak-acidic groups for ammonia separation. *ACS Sustainable Chem Eng*. 2021;9(21):7352-7360.
25. AlOmar MK, Hayyan M, Alsaadi MA, Akib S, Hayyan A, Hashim MA. Glycerol-based deep eutectic solvents: physical properties. *J Mol Liq*. 2016;215:98-103.
26. Wu XL, Sang XY, Li ZM, Tao DJ. Study on physicochemical properties and basicity of carbanion-functionalized ionic liquids. *J Mol Liq*. 2020;312:113405.
27. Tao DJ, Qu F, Li ZM, Zhou Y. Promoted absorption of CO at high temperature by cuprous-based ternary deep eutectic solvents. *AIChE J*. 2021;67(2):e17106.
28. Cui GK, Jiang K, Liu HY, et al. Highly efficient CO removal by active cuprous-based ternary deep eutectic solvents [HDEEA][cl] + CuCl + EG. *Sep Purif Technol*. 2021;274:118985.

29. Peng JJ, Xian SK, Xiao J, et al. A supported cu(I)@MIL-100 (Fe) adsorbent with high CO adsorption capacity and CO/N_2 selectivity. *Chem Eng J*. 2015;270:282-289.
30. Yin Y, Wen ZH, Shi L, et al. Cuprous/vanadium sites on MIL-101 for selective CO adsorption from gas mixtures with superior stability. *ACS Sustain Chem Eng*. 2019;7(13):11284-11292.
31. Li YX, Li SS, Xue DM, Liu XQ, Jin MM, Sun LB. Incorporation of cu(II) and selective reduction to cu(I) within confined spaces: efficient active sites for CO adsorption. *J Mater Chem A*. 2018;6(19):8930-8939.
32. Li YX, Ji YN, Jin MM, et al. Controlled construction of cu(I) sites within confined spaces via host–guest redox: highly efficient adsorbents for selective CO adsorption. *ACS Appl Mater Interfaces*. 2018;10(46):40044-40053.
33. Goodrich BF, de la Fuente JC, Gurkan BE, et al. Experimental measurements of amine-functionalized anion-tethered ionic liquids with carbon dioxide. *Ind Eng Chem Res*. 2011;50(1):111-118.
34. Xiong WJ, Shi MZ, Peng LL, Zhang XM, Hu XB, Wu YT. Low viscosity superbase protic ionic liquids for the highly efficient simultaneous removal of H_2S and CO_2 from CH_4. *Sep Purif Technol*. 2021;263:118417.
35. Huang K, Cai DN, Chen YL, Wu YT, Hu XB, Zhang ZB. Thermodynamic validation of 1-alkyl-3-methylimidazolium carboxylates as task-specific ionic liquids for H_2S absorption. *AIChE J*. 2013;59(6):2227-2235.

SUPPORTING INFORMATION

Additional supporting information may be found in the online version of the article at the publisher's website.

How to cite this article: Tao D-J, An X-C, Gao Z-T, Li Z-M, Zhou Y. Cuprous-based composite ionic liquids for the selective absorption of CO: Experimental study and thermodynamic analysis. *AIChE J*. 2022;e17631. doi:10.1002/aic.17631